

# Exact relations between macroscopic moduli of composite media in three dimensions: Application to magnetoconductivity and magneto-optics of three-dimensional composites with related columnar microstructures

Yakov M. Strelniker\*

*Minerva Center, Jack and Pearl Resnick Institute of Advanced Technology, and Department of Physics, Bar-Ilan University, IL-52900 Ramat-Gan, Israel*

David J. Bergman†

*School of Physics and Astronomy, Raymond and Beverly Sackler Faculty of Exact Sciences, Tel Aviv University, IL-69978 Tel Aviv, Israel*

(Received 10 November 2002; published 23 May 2003)

Generic three-dimensional (3D) exact relations are found between macroscopic or bulk effective moduli of composite systems with related microstructures. These relations can be established between effective values of material coefficients of the same type (e.g., conductivity and conductivity) as well as between different types of material coefficients (e.g., conductivity and permittivity). As example of possible application of these relations, a set of Keller-like quasi-3D relations are derived for the case of columnar-shaped parallel inclusions. The microstructure in the two samples can, in general, be different. In particular, exact relations between bulk effective magnetoconductivity tensor components of a pair of composite samples with interchanged constituents and different columnar microstructures (as well as between two composites with the same host but different inclusions, e.g., perfectly insulating and perfectly conducting) are found for general orientations of the applied magnetic field. Those relations are tested by comparing with a number of numerical calculations of macroscopic dc and ac response in such systems.

DOI: 10.1103/PhysRevB.67.184416

PACS number(s): 72.80.Tm, 78.66.Sq, 77.84.Lf, 73.50.Jt

## I. INTRODUCTION

The macroscopic or bulk effective moduli of a composite medium depend on its detailed microstructure, and can usually be calculated only approximately. Notwithstanding this generic feature, there exist some exact, microstructure-independent results for such moduli in the case of two-dimensional (2D) composites. These go back to a pioneering paper by Keller where it was shown that, in a 2D rectangular periodic array of inclusions, the bulk effective principal conductivities of the “phase interchanged composites”  $\sigma_{yy}^{(e)}(\sigma_1, \sigma_2)$  and  $\sigma_{zz}^{(e)}(\sigma_2, \sigma_1)$  are related in the following way:<sup>1</sup>

$$\sigma_{yy}^{(e)}(\sigma_1, \sigma_2) \sigma_{zz}^{(e)}(\sigma_2, \sigma_1) = \sigma_1 \sigma_2. \quad (1.1)$$

Here the two composites have the *same rectangular microstructure* but the two constituents, with scalar conductivities  $\sigma_1$ ,  $\sigma_2$ , have interchanged their spatial locations. The term conductivity should be understood in a broad sense of this word, i.e., it can refer to either electrical or thermal conductivity, electrical permittivity, magnetic permeability, etc. This Keller theorem (in Russian literature it is known as the Dykhne theorem<sup>2</sup>) became a powerful tool in many studies of transport problems. Thus it is no surprise that attempts were made to extend it in various ways<sup>2–11</sup> including even application to the fractional quantum Hall effect.<sup>12,13</sup> However, all of these developments were confined to the case of a strictly 2D composite (Schulgasser<sup>14</sup> and Bergman<sup>15</sup> have even proved the “nonexistence of a Keller-type theorem in three dimensions”).

Recently we have extended Keller’s theorem to a special case of three-dimensional (3D) systems with a columnar

microstructure<sup>16,17</sup> (i.e., macroscopically inhomogeneous media that are uniform in one fixed direction). Despite the fact that the geometric or structural characteristics of such a microstructure are 2D, the presence of a strong magnetic field (i.e., conductivity tensors are nonscalar) can change the character of current flow in such a system from 2D to strongly 3D, and thus invalidate the relations that were found for real 2D systems.<sup>1</sup> More specifically, we considered the case where the magnetic field is perpendicular to the columnar axis, i.e., an “in-plane” magnetic field.

Here we derive generic 3D exact relations between effective moduli of composite systems with different but related microstructures. These relations can be transformed to quasi-3D Keller-like relations when the composite has a columnar microstructure and an external magnetic field is applied in certain directions.

The remainder of this article is organized as follows. In Sec. II we summarize the required theory and write down differential equations for the local electrical potential in a pair of two-constituent composites characterized by different values of the two constituent conductivity tensors as well as different microstructures. By comparing these equations, as well as the expressions for the two macroscopic responses, we derive exact relations between the macroscopic conductivity tensors of the two problems, which hold when certain relations exist between those problems. These relations are valid for arbitrary dimensionality, and in particular for 3D composites. In Sec. III we consider a special case of 3D systems, namely a composite with columnar microstructure. For such systems we derive some Keller-like exact relations for a pair of composite samples with *interchanged phases*, and also for a pair of composites with the *same host constitu-*

ent but different types of inclusions, e.g., conductor/perfect insulator mixture and normal conductor/perfect conductor mixture. We illustrate our results by comparing them with numerical computations of magnetoconductivity in such composites. Section IV provides a summary of our main results.

## II. COORDINATE RE-SCALING AND GENERAL RELATIONS IN THREE DIMENSIONS

The electrical transport on the microscale is assumed to be describable in terms of a local curl-free electric field  $\mathbf{E}(\mathbf{r}) \equiv \nabla \phi(\mathbf{r})$  and a local divergence-free current density  $\mathbf{J}(\mathbf{r})$ , which are related to each other linearly by means of a local resistivity tensor  $\hat{\rho}(\mathbf{r})$  or a local conductivity tensor  $\hat{\sigma}(\mathbf{r}) = 1/\hat{\rho}(\mathbf{r})$ :  $\mathbf{J}(\mathbf{r}) = \hat{\sigma}(\mathbf{r}) \cdot \mathbf{E}(\mathbf{r})$ . We can express  $\hat{\sigma}(\mathbf{r})$  in terms of the constituent conductivity tensors  $\hat{\sigma}_i$  and the characteristic functions  $\theta_i(\mathbf{r})$  [ $\theta_i(\mathbf{r}) = 1$  if  $\hat{\sigma}(\mathbf{r}) = \hat{\sigma}_i$ , otherwise  $\theta_i(\mathbf{r}) = 0$ ]. In the case of a two-constituent composite medium we can write  $\hat{\sigma}(\mathbf{r}) = \hat{\sigma}_1 \theta_1(\mathbf{r}) + \hat{\sigma}_2 \theta_2(\mathbf{r}) = \hat{\sigma}_2 - \delta \hat{\sigma} \theta_1(\mathbf{r})$ ,  $\delta \hat{\sigma} \equiv \hat{\sigma}_2 - \hat{\sigma}_1$ . Using this notation, the usual differential equation  $\nabla \cdot \hat{\sigma} \cdot \nabla \phi = 0$  can be written as

$$\nabla \cdot \hat{\sigma}_2 \cdot \nabla \phi = \nabla \cdot \delta \hat{\sigma} \theta_1 \cdot \nabla \phi. \quad (2.1)$$

The local electric potential  $\phi$  can be found by solving this equation with appropriate boundary conditions.

The bulk effective or macroscopic conductivity tensor of the composite  $\hat{\sigma}_e$ , as well as the bulk effective resistivity tensor  $\hat{\rho}_e = 1/\hat{\sigma}_e$ , are defined as providing the linear relationship between the volume averages of electric field and current density  $\langle \mathbf{J} \rangle \equiv \hat{\sigma}_e \cdot \langle \nabla \phi(\mathbf{r}) \rangle$ , where  $\langle \rangle$  denotes a volume average over the entire system. From this we can write the following expression for  $\hat{\sigma}_e$ :

$$(\sigma_{\alpha\beta}^{(e)} - \sigma_{\alpha\beta}^{(2)}) = - \sum_{\gamma} \delta \sigma_{\alpha\gamma} \cdot \langle \theta_1 \nabla_{\gamma} \phi^{(\beta)} \rangle, \quad (2.2)$$

where we have introduced the notation  $\phi^{(\beta)}(\mathbf{r})$  for the electrical potential field in the composite which satisfies  $\langle \nabla \phi^{(\beta)} \rangle = \nabla r_{\beta} = \mathbf{e}_{\beta}$ , where  $\mathbf{e}_{\beta}$  is the unit vector along  $r_{\beta}$ .

We now write the partial differential equation (2.1) for two different problems: The first is characterized by the potential  $\phi$  and conductivities  $\hat{\sigma}$ ,  $\delta \hat{\sigma}$ , while the second is characterized by the potential  $\psi$  and conductivities  $\hat{\mu}$ ,  $\delta \hat{\mu}$ . In order to transform these equations into similar forms, from which we will attempt to find relations between the two problems, we execute a rescaling transformation of the Cartesian coordinates in each problem:

$$x'_{\alpha} \equiv x_{\alpha} / \sqrt{\sigma_{\alpha\alpha}^{(2)}}, \quad z'_{\alpha} \equiv z_{\alpha} / \sqrt{\mu_{\alpha\alpha}^{(2)}}. \quad (2.3)$$

It is important to note that the two rescaling transformations are different, in general. Therefore the microstructure, i.e., the shapes of the inclusions, their separations, even the symmetry, will change in different ways for the two problems. We therefore introduce the notations  $\theta'_i(\mathbf{x}')$ ,  $\Theta'_1(\mathbf{z}')$  for the characteristic or indicator functions of the rescaled

first and second problems, respectively. Equation (2.1) takes the following forms for these two problems:

$$\sum_{\alpha\beta} \frac{\sigma_{\alpha\beta}^{(2)}}{\sqrt{\sigma_{\alpha\alpha}^{(2)}\sigma_{\beta\beta}^{(2)}}} \frac{\partial^2 \phi}{\partial x'_{\alpha} \partial x'_{\beta}} = \sum_{\alpha\beta} \frac{\delta \sigma_{\alpha\beta}}{\sqrt{\sigma_{\alpha\alpha}^{(2)}\sigma_{\beta\beta}^{(2)}}} \frac{\partial}{\partial x'_{\alpha}} \left( \theta'_1 \frac{\partial \phi}{\partial x'_{\beta}} \right), \quad (2.4)$$

$$\sum_{\alpha\beta} \frac{\mu_{\alpha\beta}^{(2)}}{\sqrt{\mu_{\alpha\alpha}^{(2)}\mu_{\beta\beta}^{(2)}}} \frac{\partial^2 \psi}{\partial z'_{\alpha} \partial z'_{\beta}} = \sum_{\alpha\beta} \frac{\delta \mu_{\alpha\beta}}{\sqrt{\mu_{\alpha\alpha}^{(2)}\mu_{\beta\beta}^{(2)}}} \frac{\partial}{\partial z'_{\alpha}} \left( \Theta'_1 \frac{\partial \psi}{\partial z'_{\beta}} \right). \quad (2.5)$$

We would like to make these two equations (2.4) and (2.5) identical. That can be achieved by assuming that

$$\sigma_{\alpha\beta}^{(2)} = -\sigma_{\beta\alpha}^{(2)}, \quad \mu_{\alpha\beta}^{(2)} = -\mu_{\beta\alpha}^{(2)}, \quad \text{for } \alpha \neq \beta, \quad (2.6)$$

$$\theta'_1 = \Theta'_1, \quad (2.7)$$

$$\frac{\delta \sigma_{\alpha\beta}}{\sqrt{\sigma_{\alpha\alpha}^{(2)}\sigma_{\beta\beta}^{(2)}}} = \frac{\delta \mu_{\alpha\beta}}{\sqrt{\mu_{\alpha\alpha}^{(2)}\mu_{\beta\beta}^{(2)}}}. \quad (2.8)$$

If Eqs. (2.6)–(2.8) hold, and if the same boundary conditions (BC) are imposed upon  $\phi$  and  $\psi$ , then these two potential fields will be identical. It is clear that BC should be the same in the new, re-scaled, coordinates. However, since the values of the effective conductivities  $\hat{\sigma}_e$ ,  $\hat{\mu}_e$  are the macroscopic moduli of the samples considered, and therefore do not depend on the applied external fields or macroscopically uniform BC, we will not discuss here how BC in the re-scaled coordinate system relate to BC in the initial coordinate system. We can expect that the effective conductivity tensors  $\hat{\sigma}_e$  and  $\hat{\mu}_e$  of the unrescaled physical problems will also be equal.

Starting from Eq. (2.2) written in the new re-scaled coordinates [see Eqs. (2.3)] we get the following pair of equations:

$$\frac{\delta \sigma_{\alpha\beta}^{(e)}}{\sqrt{\sigma_{\alpha\alpha}^{(2)}\sigma_{\beta\beta}^{(2)}}} \left\langle \frac{\partial \phi^{(\beta)}}{\partial x'_{\beta}} \right\rangle = - \sum_{\gamma} \frac{\delta \sigma_{\alpha\gamma}}{\sqrt{\sigma_{\alpha\alpha}^{(2)}\sigma_{\gamma\gamma}^{(2)}}} \left\langle \theta'_1 \frac{\partial \phi^{(\beta)}}{\partial x'_{\gamma}} \right\rangle, \quad (2.9)$$

$$\frac{\delta \mu_{\alpha\beta}^{(e)}}{\sqrt{\mu_{\alpha\alpha}^{(2)}\mu_{\beta\beta}^{(2)}}} \left\langle \frac{\partial \psi^{(\beta)}}{\partial z'_{\beta}} \right\rangle = - \sum_{\gamma} \frac{\delta \mu_{\alpha\gamma}}{\sqrt{\mu_{\alpha\alpha}^{(2)}\mu_{\gamma\gamma}^{(2)}}} \left\langle \Theta'_1 \frac{\partial \psi^{(\beta)}}{\partial z'_{\gamma}} \right\rangle. \quad (2.10)$$

From these equations, together with Eq. (2.8), it now follows that the macroscopic analog of Eq. (2.8) is also valid:

$$\frac{\delta \sigma_{\alpha\beta}^{(e)}}{\sqrt{\sigma_{\alpha\alpha}^{(2)}\sigma_{\beta\beta}^{(2)}}} = \frac{\delta \mu_{\alpha\beta}^{(e)}}{\sqrt{\mu_{\alpha\alpha}^{(2)}\mu_{\beta\beta}^{(2)}}}. \quad (2.11)$$

This equation relates the macroscopic responses  $\hat{\sigma}_e$ ,  $\hat{\mu}_e$  of a pair of two-constituent composite media which differ in their microstructure [ $\theta_1(\mathbf{r})$  vs  $\Theta_1(\mathbf{r})$ ] as well as in their constituent physical (electrical) properties.

This result can be easily extended to the case of multiconstituent composites, including the extreme case where the local conductivities depend continuously on the coordinates.

The pair of microstructures under consideration are related to each other by the coordinate rescaling transformation of Eq. (2.3). Thus, if  $L_\alpha$  is a characteristic size in the direction  $\alpha$  in the first system and  $\mathcal{L}_\alpha$  is the analogous value in the second system, then these lengths will be related to each other by

$$\mathcal{L}_\alpha = L_\alpha \sqrt{\mu_{\alpha\alpha}^{(2)}/\sigma_{\alpha\alpha}^{(2)}}. \quad (2.12)$$

If the tensors  $\hat{\sigma}_2$  and  $\hat{\mu}_2$  have diagonal elements which are not proportional to each other, then an initial spherical shape of inclusions will be transformed to an ellipsoidal shape. In particular cases, however, it is possible to have a situation where the shapes of inclusions remain unchanged, i.e.,  $\mathcal{L}_\alpha/\mathcal{L}_\beta = L_\alpha/L_\beta$  ( $\alpha \neq \beta$ ).

We would like to emphasize that the relations (2.11) are established between two samples with microstructures that differ in a nonarbitrary fashion: The shapes of the microstructures in the two samples are related via Eqs. (2.3), (2.7), and (2.12). In particular, the rescaling transformation (2.3) alters not only the inclusion sizes, but also other characteristic lengths (such as the distance between inclusions, macroscopic size of the composite sample, etc). However, the volume fraction of each constituent remains the same.

Both Eq. (2.8) and Eq. (2.11) are simplified when  $\alpha = \beta$ , or if we assume

$$\frac{\sigma_{\alpha\beta}^{(2)}}{\sqrt{\sigma_{\alpha\alpha}^{(2)}\sigma_{\beta\beta}^{(2)}}} = \frac{\mu_{\alpha\beta}^{(2)}}{\sqrt{\mu_{\alpha\alpha}^{(2)}\mu_{\beta\beta}^{(2)}}}. \quad (2.13)$$

In those cases we get

$$\frac{\sigma_{\alpha\beta}^{(1)}}{\sqrt{\sigma_{\alpha\alpha}^{(2)}\sigma_{\beta\beta}^{(2)}}} = \frac{\mu_{\alpha\beta}^{(1)}}{\sqrt{\mu_{\alpha\alpha}^{(2)}\mu_{\beta\beta}^{(2)}}}, \quad (2.14)$$

$$\frac{\sigma_{\alpha\beta}^{(e)}}{\sqrt{\sigma_{\alpha\alpha}^{(2)}\sigma_{\beta\beta}^{(2)}}} = \frac{\mu_{\alpha\beta}^{(e)}}{\sqrt{\mu_{\alpha\alpha}^{(2)}\mu_{\beta\beta}^{(2)}}}. \quad (2.15)$$

The latter equations can be re-written in terms of the macroscopic resistivity tensor ( $\hat{\rho}_e \equiv 1/\hat{\sigma}_e$ ,  $\hat{\nu}_e \equiv 1/\hat{\mu}_e$ ) components

$$\rho_{\alpha\beta}^{(e)} = \nu_{\alpha\beta}^{(e)} \sqrt{\frac{\mu_{\alpha\alpha}^{(2)}\mu_{\beta\beta}^{(2)}}{\sigma_{\alpha\alpha}^{(2)}\sigma_{\beta\beta}^{(2)}}}. \quad (2.16)$$

In order to verify the relations (2.11), we present in Fig. 1 the results of our numerical calculations<sup>18</sup> on a composite sample with host conductivity  $\hat{\sigma}_2$  and a periodic simple cubic array of spherical inclusions with conductivity  $\hat{\sigma}_1$ , where  $\hat{\sigma}_1 = 10\hat{I}$ ,  $\hat{\sigma}_2 = \hat{I}$  ( $\hat{I}$  is the unit matrix). Also shown are calculations on another composite with constituent conductivities  $\hat{\mu}_1$ ,  $\hat{\mu}_2$ . The tensors  $\hat{\mu}_1$  and  $\hat{\mu}_2$  are not arbitrary but are connected through Eqs. (2.6)–(2.8) with the local conduc-

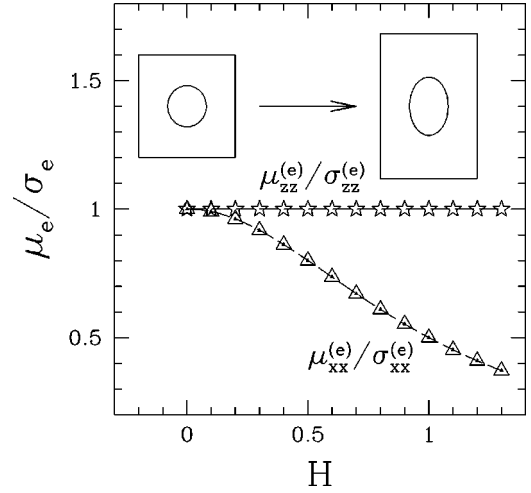


FIG. 1. Illustration of the exact relations (2.11): Ratios of the  $zz$  and  $xx$  components of the macroscopic conductivities  $\hat{\sigma}_e$  and  $\hat{\mu}_e$  of a pair of composite samples where the constituent conductivities and microstructure are related by Eqs. (2.6)–(2.12). The inclusions in the  $\hat{\sigma}$  system are a simple cubic array of identical spheres with radius  $R=0.3a$  ( $a$  is the cubic lattice constant), while the inclusions in the  $\hat{\mu}$  system are a rectangular-prismatic array of spheroids with sizes chosen in accordance with Eq. (2.3) and conductivity  $\hat{\mu}$ . Note that the aspect ratio of the spheroids in the latter sample, as well as that of the prismatic unit cells, depend on the magnetic field strength  $H$ . Therefore the aspect ratio varies along the  $H$  axis of the figure, as indicated by the insets. The stars and triangles represent the ratios  $\mu_{zz}^{(e)}/\sigma_{zz}^{(e)}$ ,  $\mu_{xx}^{(e)}/\sigma_{xx}^{(e)}$  as obtained by numerical calculations, while the dashed lines depict the ratios of the constituent conductivities  $\mu_{xx}^{(2)}/\sigma_{xx}^{(2)}$  and  $\mu_{zz}^{(2)}/\sigma_{zz}^{(2)}$ , in accordance with the predictions of Eq. (2.11). The host and inclusions of the  $\hat{\sigma}$  system are characterized by constituent conductivity tensors which are scalars  $\hat{\sigma}_2 = \hat{I}$  ( $\hat{I}$  is the unit matrix) and  $\hat{\sigma}_1 = 10\hat{I}$ . The host conductivity of the  $\hat{\mu}$  system is taken to have a free electron form (A2) with Ohmic resistivity equal to 1 and  $\mathbf{B}$  directed along the  $z$  axis. In that case  $\hat{\mu}_1$  is determined by Eq. (2.8).

ivities  $\hat{\sigma}_1$ ,  $\hat{\sigma}_2$  in the first system. For example, we can take the conductivity tensor  $\hat{\mu}_2$  to have the form of a free-electron conductivity tensor—see Eq. (A2) in Appendix A. In that case  $\hat{\mu}_1$  is determined by Eq. (2.8). Since  $\hat{\mu}_2$  of Eq. (A2) usually has unequal diagonal elements when  $\mathbf{B} \neq 0$ , therefore the shape of the  $\hat{\mu}_1$  inclusions will be ellipsoidal—see Eq. (2.12). The numerical calculations are in agreement with our previous predictions.

The relations formulated here establish connections between macroscopic moduli of physical properties whose local behavior is described by a differential equation like Eq. (2.1). This means that not only electrical conductivities obey those relations, but also electrical permittivities, thermal conductivities, and magnetic permeabilities.

### III. APPLICATION TO COMPOSITES WITH A COLUMNAR MICROSTRUCTURE

The exact relations found in the previous section are valid for 3D composite media. We believe these relations will have

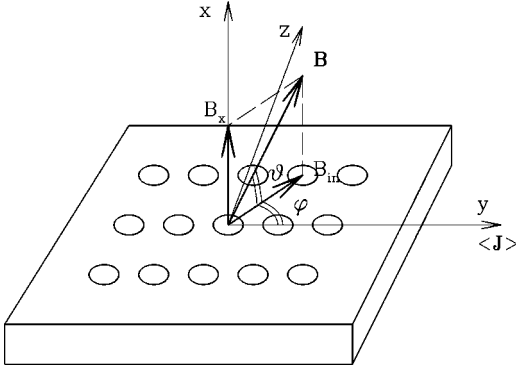


FIG. 2. Composite conductor with columnar microstructure shaped as a thin film, with magnetic field  $\mathbf{B}$  tilted with respect to the film plane.  $\vartheta$  is the angle between  $\mathbf{B}$  and the film plane, while  $\varphi$  is the angle between the planar projection of  $\mathbf{B}$ ,  $B_{in}$ , and the volume averaged current density  $\langle \mathbf{J} \rangle$ , which is perpendicular to the columnar axis  $x$ .

a broad range of applications in different branches of physics. In order to illustrate the consequences and power of these relations, we apply them here to the problem of magnetoconductance and magnetoresistance in composites with a columnar microstructure, i.e., we consider a heterogeneous medium, characterized by a local resistivity tensor that depends only upon  $y$  and  $z$ . This is a 3D medium with 2D heterogeneity, with the  $x$  axis as columnar symmetry axis—see Fig. 2. We note that, in spite of the 2D character of heterogeneity, the transport processes will, in general, be three dimensional, i.e., the local current density  $\mathbf{J}(\mathbf{r})$  will usually have a nonzero component along the columnar symmetry axis  $x$  whenever  $\mathbf{B}$  has a nonvanishing component in the  $y, z$  plane (the “in-plane” component)  $B_{in} \neq 0$ , even if the macroscopic or volume averaged current density  $\langle \mathbf{J} \rangle$  is perpendicular to  $x$ .

Although columnar microstructures are special, i.e., they are not generic 3D microstructures, they are nevertheless very common and very important, especially in fiber reinforced composites and also in various types of heterogeneous thin films. In particular, a thin film with a periodic columnar microstructure, such as a periodic array of perpendicular cylindrical etched holes, is easier to fabricate than any 3D periodic array.<sup>23,24</sup>

In Refs. 16, 17, 25, and 26 it was shown that, in a composite with a columnar microstructure, the electrical transport in the plane perpendicular to the columnar axis can be treated separately from the transport in other directions. In particular, if  $x$  is the columnar axis, then the  $y, z$  components of  $\hat{\sigma}_e$ ,  $\hat{\mu}_e$  only depend on the  $y, z$  components of the constituent tensors  $\hat{\sigma}_i$ ,  $\hat{\mu}_i$ , and they can be calculated by implementing the 2D version of Eqs. (2.1) and (2.2) in the  $y, z$  plane—see Appendix B. In that plane, the classical duality symmetry of Dykhne<sup>2</sup> is valid, which leads to Mendelson’s generalization of Keller’s theorem for 2D systems.<sup>3,4</sup> This is now exploited by using the dual tensors  $\hat{\mu}_d^{(i)} \equiv \hat{\mu}_i^T / \det_{2D} \hat{\mu}_i$ ,  $i=1,2$  ( $\hat{\mu}_i^T$  denotes the transposed matrix of  $\hat{\mu}_i$ ) in place of  $\hat{\mu}_i$  in Eqs. (2.13) and (2.14). In this way we get the following expressions:

$$\frac{\mu_{zy}^{(2)} / \det_{2D} \hat{\mu}_2}{\sqrt{\mu_{yy}^{(2)} \mu_{zz}^{(2)} / (\det_{2D} \hat{\mu}_2)^2}} = \frac{\sigma_{yz}^{(2)}}{\sqrt{\sigma_{yy}^{(2)} \sigma_{zz}^{(2)}}}, \quad (3.1)$$

$$\frac{\mu_{yy}^{(1)} / \det_{2D} \hat{\mu}_1}{\mu_{yy}^{(2)} / \det_{2D} \hat{\mu}_2} = \frac{\sigma_{yy}^{(1)}}{\sigma_{yy}^{(2)}}, \quad (3.2)$$

$$\frac{\mu_{zz}^{(1)} / \det_{2D} \hat{\mu}_1}{\mu_{zz}^{(2)} / \det_{2D} \hat{\mu}_2} = \frac{\sigma_{zz}^{(1)}}{\sigma_{zz}^{(2)}}, \quad (3.3)$$

$$\frac{\mu_{zy}^{(1)} / \det_{2D} \hat{\mu}_1}{\sqrt{\mu_{yy}^{(2)} \mu_{zz}^{(2)} / (\det_{2D} \hat{\mu}_2)^2}} = \frac{\sigma_{yz}^{(1)}}{\sqrt{\sigma_{yy}^{(2)} \sigma_{zz}^{(2)}}}, \quad (3.4)$$

$$\frac{\mu_{\alpha\beta}^{(e)} / \det_{2D} \hat{\mu}_e}{\sqrt{\mu_{\alpha\alpha}^{(2)} \mu_{\beta\beta}^{(2)} / (\det_{2D} \hat{\mu}_2)^2}} = \frac{\sigma_{\alpha\beta}^{(e)}}{\sqrt{\sigma_{\alpha\alpha}^{(2)} \sigma_{\beta\beta}^{(2)}}}. \quad (3.5)$$

Equations (3.1)–(3.4) cannot be solved in a unique fashion for  $\hat{\mu}_1$  and  $\hat{\mu}_2$ . On the other hand, some unique explicit forms for  $\hat{\mu}_1$  and  $\hat{\mu}_2$  can be obtained by splitting each of the Eqs. (3.2)–(3.4) into two parts. This can be done in different ways, leading to different types of exact relations among elements of the macroscopic moduli  $\hat{\sigma}_e$  and  $\hat{\mu}_e$ .

#### A. Relations for composites with the same microstructures and hosts but different inclusion properties

We first consider samples where the 2D host medium is the same. This means that  $\mu_{yy}^{(2)} = \sigma_{yy}^{(2)}$  and  $\mu_{zz}^{(2)} = \sigma_{zz}^{(2)}$ . Equation (3.1) will then hold automatically, if we also assume that  $\mu_{zy}^{(2)} = \sigma_{yz}^{(2)}$ , due to Eq. (2.6). Therefore we can write

$$\hat{\mu}_{2D}^{(2)} = \begin{pmatrix} \sigma_{yy}^{(2)} & \sigma_{zy}^{(2)} \\ \sigma_{yz}^{(2)} & \sigma_{zz}^{(2)} \end{pmatrix} = \begin{pmatrix} \sigma_{yy}^{(2)} & -\sigma_{yz}^{(2)} \\ -\sigma_{zy}^{(2)} & \sigma_{zz}^{(2)} \end{pmatrix}. \quad (3.6)$$

This can be realized trivially when  $\mu_{yz}^{(2)} = \mu_{zy}^{(2)} = \sigma_{yz}^{(2)} = \sigma_{zy}^{(2)} = 0$ , which in the free-electron model [see Eq. (A2)] corresponds to the case  $H_{2x}^{(\mu)} = H_{2x}^{(\sigma)} = 0$ ,  $H_{2y}^{(\mu)} H_{2z}^{(\mu)} = H_{2y}^{(\sigma)} H_{2z}^{(\sigma)} = 0$ , discussed in Refs. 16 and 17. However, Eq. (3.6) can be also realized when  $H_{2x}^{(\mu)} = -H_{2x}^{(\sigma)}$  and  $H_{2y}^{(\mu)} H_{2z}^{(\mu)} = -H_{2y}^{(\sigma)} H_{2z}^{(\sigma)}$ . That is, we keep the host in the  $\hat{\mu}$  system the same as it was in the  $\hat{\sigma}$  system, but reverse signs of the appropriate field components

The form of the conductivity tensor of the other constituent, namely the inclusions,  $\hat{\mu}_1$ , can be found from Eqs. (3.2)–(3.4):

$$\hat{\mu}_{2D}^{(1)} = \frac{\det_{2D} \hat{\mu}_1}{\det_{2D} \hat{\mu}_2} \hat{\sigma}_{2D}^{(1)}, \quad (3.7)$$

where all the tensors and determinants should be understood as 2D (in the  $y, z$  plane). Constructing from this the 2D determinant  $\det_{2D} \hat{\mu}_1$ , we find that



$$\det_{2D}\hat{\mu}_1 = \frac{(\det_{2D}\hat{\sigma}_2)^2}{\det_{2D}\hat{\sigma}_1}. \quad (3.8)$$

Therefore Eq. (3.7) can also be written in the form

$$\hat{\mu}_{2D}^{(1)} = \frac{\det_{2D}\hat{\sigma}_2 \hat{\sigma}_{2D}^{(1)}}{\det_{2D}\hat{\sigma}_1}. \quad (3.9)$$

The relation between the in-plane elements of  $\hat{\sigma}_e$  and  $\hat{\mu}_e$  can be written in the following explicit form

$$\sigma_{yy}^{(e)} \left( \mu_{zz}^{(e)} - \frac{\mu_{yz}^{(e)} \mu_{zy}^{(e)}}{\mu_{yy}^{(e)}} \right) \quad (3.10)$$

$$= \sigma_{zz}^{(e)} \left( \mu_{yy}^{(e)} - \frac{\mu_{yz}^{(e)} \mu_{zy}^{(e)}}{\mu_{zz}^{(e)}} \right) \quad (3.11)$$

$$= -\sigma_{zy}^{(e)} \left( \mu_{yz}^{(e)} - \frac{\mu_{yy}^{(e)} \mu_{zz}^{(e)}}{\mu_{zy}^{(e)}} \right) \quad (3.12)$$

$$= -\sigma_{yz}^{(e)} \left( \mu_{zy}^{(e)} - \frac{\mu_{yy}^{(e)} \mu_{zz}^{(e)}}{\mu_{yz}^{(e)}} \right) = \det_{2D}\hat{\sigma}_2. \quad (3.13)$$

Note that, since  $\sigma_{yy}^{(2)} = \mu_{yy}^{(2)}$ ,  $\sigma_{zz}^{(2)} = \mu_{zz}^{(2)}$ , the sizes of the inclusions in the  $\hat{\mu}$  system are the same as in the  $\hat{\sigma}$  system.

The relations derived here are generalizations of those found in Ref. 16: The magnetic field is no longer restricted to lie in the  $y, z$  plane.

### B. Relations for composites with different microstructures and different constituents

It is possible to get other types of exact relations from Eqs. (3.2)–(3.4). The expression for  $\sigma_{zy}^{(1)}$  follows directly from Eq. (3.4), while  $\sigma_{yy}^{(1)}$ ,  $\sigma_{zz}^{(1)}$  can be found as a result of a different non-trivial splitting of Eqs. (3.2) and (3.3). We can, for example, assume that the numerators of the lhs of Eqs. (3.2) and (3.3) are equal to the denominators on the right-hand side of these equations and vice versa. In this way we get

$$\frac{\mu_{yy}^{(1)}}{\det_{2D}\hat{\mu}_1} = \frac{1}{\sigma_{yy}^{(2)}}, \quad (3.14)$$

$$\frac{\mu_{zz}^{(1)}}{\det_{2D}\hat{\mu}_1} = \frac{1}{\sigma_{zz}^{(2)}}, \quad (3.15)$$

$$\frac{\mu_{yz}^{(1)}}{\det_{2D}\hat{\mu}_1} = \frac{\sigma_{zy}^{(1)}}{\det_{2D}\hat{\mu}_2} \sqrt{\frac{\mu_{yy}^{(2)} \mu_{zz}^{(2)}}{\sigma_{zz}^{(2)} \sigma_{yy}^{(2)}}}, \quad (3.16)$$

$$\frac{\mu_{yy}^{(2)}}{\det_{2D}\hat{\mu}_2} = \frac{1}{\sigma_{yy}^{(1)}}, \quad (3.17)$$

$$\frac{\mu_{zz}^{(2)}}{\det_{2D}\hat{\mu}_2} = \frac{1}{\sigma_{zz}^{(1)}}, \quad (3.18)$$

$$\frac{\mu_{yz}^{(2)}}{\det_{2D}\hat{\mu}_2} = \frac{\sigma_{zy}^{(2)}}{\det_{2D}\hat{\mu}_2} \sqrt{\frac{\mu_{yy}^{(2)} \mu_{zz}^{(2)}}{\sigma_{zz}^{(2)} \sigma_{yy}^{(2)}}}. \quad (3.19)$$

Constructing the 2D determinants from these equations, we obtain

$$\det_{2D}\hat{\mu}_1 = \frac{\sigma_{yy}^{(2)} \sigma_{zz}^{(2)} \sigma_{yy}^{(1)} \sigma_{zz}^{(1)}}{\det_{2D}\hat{\sigma}_1}, \quad (3.20)$$

$$\det_{2D}\hat{\mu}_2 = \frac{\sigma_{yy}^{(1)} \sigma_{zz}^{(1)} \sigma_{yy}^{(2)} \sigma_{zz}^{(2)}}{\det_{2D}\hat{\sigma}_2}. \quad (3.21)$$

Substituting these back into Eqs. (3.14)–(3.19), we get

$$\hat{\mu}_{2D}^{(1)} = \frac{\sigma_{yy}^{(1)} \sigma_{zz}^{(1)}}{\det_{2D}\hat{\sigma}_1} \begin{pmatrix} \sigma_{zz}^{(2)} & \frac{\sigma_{zy}^{(1)} \sqrt{\sigma_{yy}^{(2)} \sigma_{zz}^{(2)}}}{\sqrt{\sigma_{yy}^{(1)} \sigma_{zz}^{(1)}}} \\ \frac{\sigma_{yz}^{(1)} \sqrt{\sigma_{yy}^{(2)} \sigma_{zz}^{(2)}}}{\sqrt{\sigma_{yy}^{(1)} \sigma_{zz}^{(1)}}} & \sigma_{yy}^{(2)} \end{pmatrix}, \quad (3.22)$$

and a similar expression for  $\hat{\mu}_{2D}^{(2)}$ , where the subscripts 1 and 2 should be interchanged. Thus each of the conductivity tensors  $\hat{\mu}_1$  and  $\hat{\mu}_2$  depends on both of the constituent conductivities  $\hat{\sigma}_1$  and  $\hat{\sigma}_2$ . If  $\hat{\sigma}_1$  and  $\hat{\sigma}_2$  are taken to have the free-electron form of Eq. (A2), with  $\mathbf{B}$  directed along  $z$ , i.e.,  $\sigma_{yz}^{(i)} = \sigma_{zy}^{(i)} = 0$ ,  $i = 1, 2$ , then the  $y, z$  components of  $\hat{\mu}_1$  and  $\hat{\mu}_2$  simplify to

$$\hat{\mu}_{2D}^{(1)} = \frac{1}{\rho_0^{(2)}(1+H_2^2)} \begin{pmatrix} 1+H_2^2 & 0 \\ 0 & 1 \end{pmatrix}, \quad (3.23)$$

$$\hat{\mu}_{2D}^{(2)} = \frac{1}{\rho_0^{(1)}(1+H_1^2)} \begin{pmatrix} 1+H_1^2 & 0 \\ 0 & 1 \end{pmatrix}. \quad (3.24)$$

Since there are no restrictions on the other tensor components of  $\hat{\mu}_e$ , those can be chosen so as to make the entire 3D tensors  $\hat{\mu}_1$ ,  $\hat{\mu}_2$  free-electron like. That means taking  $\mu_{xx} = 1/\rho_0(1+H^2)$ ,  $\mu_{yx} = -\mu_{xy} = H\mu_{xx}$ ,  $\mu_{yz} = \mu_{zy} = 0$ . When constructed in this fashion, the 3D tensors  $\hat{\mu}_1$  and  $\hat{\mu}_2$  correspond to free-electron conductors with  $\mathbf{B} \parallel y$ , i.e., rotated by  $90^\circ$  with respect to  $\mathbf{B}$  in the  $\hat{\sigma}$  system. Recalling that this entire discussion is also based on the duality symmetry, we should not be surprised to find that the exact relations which follow involve a pair of composites with *interchanged constituents*, as in the case of the 2D Keller expression (1.1), but with the magnetic field rotated by  $90^\circ$ .

Taking into account Eqs. (3.14)–(3.21), we obtain the following relations from Eq. (2.11):

$$\sigma_{yy}^{(e)} \left( \mu_{zz}^{(e)} - \frac{\mu_{zy}^{(e)} \mu_{yz}^{(e)}}{\mu_{yy}^{(e)}} \right) = \sigma_{yy}^{(1)} \sigma_{yy}^{(2)}, \quad (3.25)$$

$$\sigma_{zz}^{(e)} \left( \mu_{yy}^{(e)} - \frac{\mu_{yz}^{(e)} \mu_{zy}^{(e)}}{\mu_{zz}^{(e)}} \right) = \sigma_{zz}^{(1)} \sigma_{zz}^{(2)}, \quad (3.26)$$

$$\begin{aligned} -\sigma_{yz}^{(e)} \left( \mu_{zy}^{(e)} - \frac{\mu_{yy}^{(e)} \mu_{zz}^{(e)}}{\mu_{yz}^{(e)}} \right) &= -\sigma_{zy}^{(e)} \left( \mu_{yz}^{(e)} - \frac{\mu_{yy}^{(e)} \mu_{zz}^{(e)}}{\mu_{yz}^{(e)}} \right) \\ &= \sqrt{\sigma_{yy}^{(1)} \sigma_{zz}^{(1)} \sigma_{yy}^{(2)} \sigma_{zz}^{(2)}}. \end{aligned} \quad (3.27)$$

Since  $\hat{\mu}_2 \neq \hat{\sigma}_2$ , it follows from Eq. (2.12) that the inclusions in the  $\hat{\mu}$  system are compressed by different factors in different directions.

Naturally, Eqs. (3.25)–(3.27) can be translated into exact relations among the different components of the macroscopic resistivity tensors  $\hat{\rho}_e \equiv 1/\hat{\sigma}_e$  and  $\hat{\nu}_e \equiv 1/\hat{\mu}_e$ . In the general case, the forms of the relations written in terms of  $\hat{\rho}_e$ ,  $\hat{\nu}_e$  are more complicated than the expressions given above in terms of  $\hat{\sigma}_e$ ,  $\hat{\mu}_e$ . Moreover, these more complicated expressions will usually involve components of  $\hat{\rho}_e$ ,  $\hat{\nu}_e$  other than just the  $y, z$ -plane components. Only in the special case of isotropic constituents with a magnetic field perpendicular to the columnar axis  $\mathbf{B} \perp x$  were simple relations obtained in terms of  $\hat{\rho}_e$ ,  $\hat{\nu}_e$ —see Ref. 28.

The relations between the macroscopic responses of a  $\hat{\sigma}$  system and a  $\hat{\mu}$  system with “interchanged” constituents and different microstructures were checked numerically for the pairs of two-constituent composite samples shown in Fig. 3. The  $\hat{\sigma}$  sample was taken to be a free-electron host medium with metallic cylindrical inclusions as a periodic square lattice. (By “metallic,” as opposed to “semiconducting,” we mean conductors for which the Hall and other nondiagonal components of  $\hat{\sigma}$  are negligible, therefore the conductivity tensor is well approximated by a scalar  $\hat{\sigma} = \sigma_0 \hat{I}$ .) The  $\hat{\mu}$  sample is a composite where the host is metallic, while the inclusions are characterized by a semiconducting free-electron conductivity with nonzero magnetic field  $\mathbf{B}$ . The shape of the inclusions, as well as other characteristic sizes in the  $\hat{\mu}$  sample should differ from the corresponding sizes in the  $\hat{\sigma}$  system, in accordance with Eq. (2.3).

### C. ac case

The above discussion remains valid if we reinterpret divergence equation  $\nabla \cdot \mathbf{J} = 0$  as referring to the electrical displacement field  $\mathbf{D} = \hat{\epsilon}(\mathbf{r}) \cdot \mathbf{E}$ , where  $\hat{\epsilon}(\mathbf{r})$  is position dependent tensor of electrical permittivity, instead of to the current density  $\mathbf{J}$ . Instead of Eq. (2.1) we will then have  $\nabla \cdot \hat{\epsilon}(\mathbf{r}) \cdot \nabla \phi = 0$ . This means that all the conductivity tensors  $\hat{\sigma}$  get replaced by electrical permittivity tensors  $\hat{\epsilon}$ , which in the quasistatic regime can be written as  $\hat{\epsilon} = \epsilon_0 \hat{I} + i(4\pi/\omega)\hat{\sigma}$ , where  $\omega$  is the angular frequency,  $\epsilon_0$  is the scalar dielectric

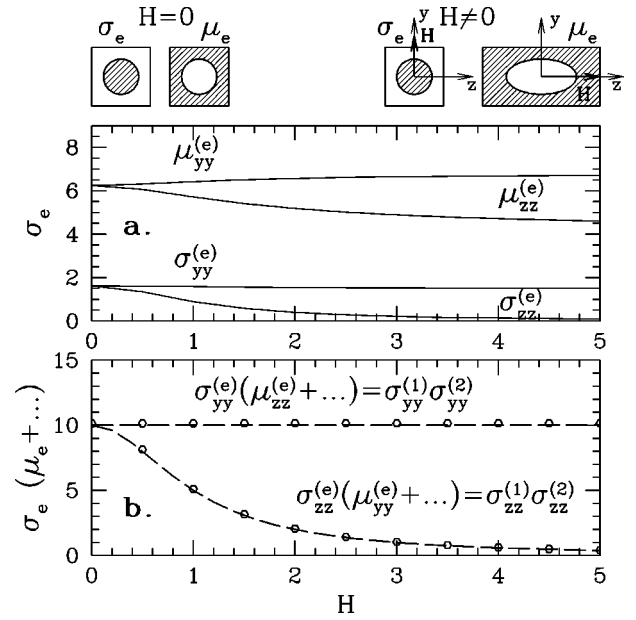


FIG. 3. Illustrations of the exact relations (3.25) and (3.26) for a pair of composite samples with “interchanged” constituents. (a)  $yy$  and  $zz$  components of the macroscopic conductivity tensors  $\hat{\sigma}_e$  and  $\hat{\mu}_e$  vs  $H$ . The  $\hat{\mu}$  system is obtained from the  $\hat{\sigma}$  system by interchanging the constituents and rescaling the coordinate axes in an isotropic fashion. (b) The combinations (3.25) and (3.26): Open circles are the values obtained by numerical computations, while the dashed lines are theoretical curves. Top: Sketch of the unit cells of the periodic composites used in our calculations. In the  $\hat{\sigma}$  sample the host (shown as white area) is a free-electron conductor characterized by Eq. (A2) with  $\rho_0=1$  and  $\mathbf{B}$  directed along  $y$ , while the inclusions (shown as a dashed area) are a square array of parallel metallic circular cylinders, with axes along  $x$ , scalar conductivity tensor  $\hat{\sigma}_1 = 10\hat{I}$  [therefore  $\sigma_{yy}^{(1)}\sigma_{yy}^{(2)} = 10$ ,  $\sigma_{zz}^{(1)}\sigma_{zz}^{(2)} = 10/(1+H^2)$ ] and radius  $R=0.3a$ , where  $a$  is the lattice parameter of the square array. The  $\hat{\mu}$  sample is obtained by interchanging the constituents, rescaling the coordinate axes, and performing the duality transformation. The host is now metallic with  $\hat{\mu}_2 = \hat{\sigma}_1$ , and the inclusions are free-electron conductors with  $\hat{\mu}_1$  having a form similar to  $\hat{\sigma}_2$  but with the magnetic field along  $z$ , i.e., rotated by  $90^\circ$  in the  $y, z$  plane. The inclusion shapes and sizes, as well as the lattice (inclusion array) parameters, are transformed in accordance with Eq. (2.3). Note that the inclusion sizes and other characteristic lengths in the  $\hat{\mu}$  system keep changing with  $H$ . The dependence of  $\mu_{yy}^{(e)}$  and  $\mu_{zz}^{(e)}$  on  $H$  [see (a)] reflects those changes, thus it cannot be understood as simple magnetoconductivity in a free-electron conductor, which would arise from inverting a resistivity matrix where only the Hall components depend upon  $H$ .

constant of the background ionic lattice,  $\hat{I}$  is the unit tensor, and  $\hat{\sigma}$  is the ac conductivity tensor [see Appendix A, Eq. (A3), and Refs. 29–31].

Relations (3.25)–(3.27) can then be easily rewritten for the ac case by replacing each of the conductivity tensors  $\hat{\sigma}$  by an electrical permittivity tensor  $\hat{\epsilon}$ . Otherwise we retain our previous definitions and expressions for  $\hat{\mu}$ . In particular, relations (3.25)–(3.27) can be used in order to connect two

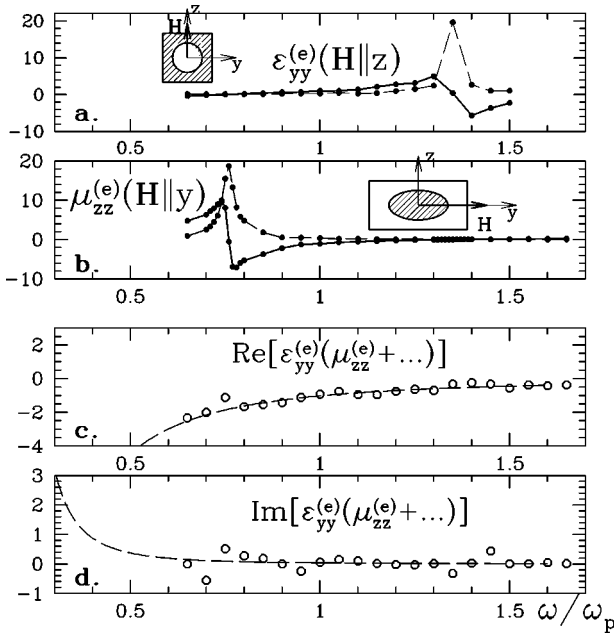


FIG. 4. (a) and (b): Plots of the real (solid lines) and imaginary (dashed lines) parts of the  $yy$  and  $zz$  components of the macroscopic electrical permittivity tensors  $\hat{\epsilon}_e$  and  $\hat{\mu}_e$  vs the dimensionless frequency  $\omega/\omega_p$  ( $\omega_p$  is the plasma frequency of the metallic constituent—see Appendix A). (c) and (d): Real and imaginary parts of the combination (3.25) with  $\hat{\sigma}$  replaced by  $\hat{\epsilon}$ . The predicted values are shown as dashed lines, while the values obtained from numerical computations are shown as open circles. Insets: Sketches of the unit cells of the periodic composites used in our calculations. In the  $\hat{\epsilon}$  sample [see (a)] the host (shown as shaded area) is a free-electron conductor characterized by Eq. (A3) with  $\mathbf{B}$  directed along  $z$ , while the inclusions (shown as a white area) are a square array of parallel dielectric circular cylinders with axes along  $x$ ,  $\hat{\epsilon} = \hat{I}$ , and radius  $R = 0.3a$ , where  $a$  is the lattice parameter of the square array. The  $\hat{\mu}$  sample is obtained by interchanging the constituents, rescaling the coordinate axes, and performing the duality transformation. The host is now a dielectric with  $\hat{\mu}_2 = \hat{I}$  and the inclusions are free-electron conductors with  $\hat{\mu}_1$  similar to Eq. (A3) but with the magnetic field along  $y$ , i.e., rotated by  $90^\circ$  in the  $y, z$  plane. The inclusion shapes, as well as all the characteristic lengths in the  $\hat{\mu}$  system are changed in accordance with Eq. (2.12). The following values were used in constructing  $\hat{\mu}_1$  [see Eq. (A3)]:  $\tau\omega_p = 30$ ,  $\omega/\omega_p \sim 1$ ,  $\epsilon_0 = 0$ .

different situations: A system  $\hat{\epsilon}$  of conducting host with an array of insulating inclusions and a system  $\hat{\mu}$  of insulating host with an array of conducting inclusions. In Fig. 4 we plot directly computed components of the macroscopic permittivity tensors  $\hat{\epsilon}_e$ ,  $\hat{\mu}_e$  of two such systems vs the frequency  $\omega$ , and also of combinations of those components corresponding to Eq. (3.25) vs  $\omega$ . The latter combinations are compared to the values predicted by the right-hand side of that equation. The so-called surface plasmon resonances (shifted by presence of the magnetic field) can be seen at frequencies  $\omega = \omega_{res}(H)$ —expressions for these frequencies are given in Refs. 29–31. The shape of the inclusions is changed in accordance with Eq. (2.12). In order not to deal with rescaling

transformations involving complex valued lengths (note that  $\hat{\epsilon}$  and  $\hat{\mu}$  are now complex valued tensors), we consider the limit  $\omega\tau \gg 1$ , when  $1 - i\omega\tau \approx i\omega\tau$  (here  $\tau$  is the conductivity relaxation time—see Appendix A). The characteristic sizes in the  $\hat{\mu}$  system will then be related to the sizes in the  $\hat{\epsilon}$  system by  $\mathcal{L}_y \cong L_y / \sqrt{\epsilon + \omega_p^2 \tau^2 / (H^2 - \omega^2 \tau^2)}$ ,  $\mathcal{L}_z \cong L_z \sqrt{\epsilon + \omega_p^2 / \omega^2}$ . This simplification of what would have otherwise been a complex coordinate rescaling transformation [see Eq. (2.3)] leads to substantial deviations of the computed results from theoretical predictions only in a narrow interval of frequencies near each of the surface plasmon resonances  $\omega_{res}(H)$ . In all other frequency domains there is good agreement between the two sets of values. In order to achieve better agreement (especially near the surface plasmon resonances) a more careful calculation should be performed, which does not ignore the nonreal nature of the rescaling transformation. This will be described elsewhere. Note that for  $\mathbf{B} \parallel z$  and  $\mathbf{B} \parallel y$ , the off-diagonal components  $\mu_{yz}^{(e)}$ ,  $\mu_{zy}^{(e)}$  vanish, therefore the combination which appears on the rhs of Eq. (3.25) reduces to the product  $\epsilon_{yy}^{(e)} \mu_{zz}^{(e)}$ .

#### IV. SUMMARY

*Exact relations* were found among elements of the macroscopic or bulk effective conductivity tensors of pairs of two-constituent composites. These relations are valid even when those elements have quite general values, i.e., nonscalar, nonsymmetric, and nonreal. Since these relations follow directly from a comparison of different differential equations and are not connected with any duality transformation, they are valid for systems of arbitrary dimensionality. They can relate between composites with different microstructures, and even between different physical moduli of different composites: They can relate between the macroscopic conductivities of two composites with different microgeometries as well as with different constituent properties, and they can also relate between electrical conductivity and electrical permittivity or thermal conductivity, etc.

In the special case of composites with a columnar microstructure, quasi-3D generalizations of the Keller relations can be obtained from the above described relations by invoking the duality symmetry. These apply to pairs of composites with interchanged constituents as well as to pairs of composites with different microgeometries.

Both the generic 3D exact relations and the quasi-3D generalizations of Keller's relations were tested against numerical computations. In the case of ac electrical permittivity, the relations that were found can be used to make connections between different types of physical phenomena. For example, the magneto-optical response of a conducting thin film with an array of subwavelength holes, where extraordinary light transmission has been observed,<sup>29,32</sup> can be related to the magneto-optical response of an array of parallel conducting sticks embedded in a dielectric host, which are being studied and discussed extensively as systems where negative electrical permittivity and negative magnetic permeability are attainable simultaneously.<sup>33–36</sup> Magneto-optical response of such arrays of parallel conducting sticks are also being

studied in connection with other interesting modes of behavior.<sup>30,31,37,38</sup>

Experimental tests of the relations presented in this paper for both dc and ac response would also be desirable. The applicability of the generalized Keller relations is not restricted to columnar systems of infinite thickness. Finite thickness films will also satisfy it very well if the film thickness  $\ell$ , heterogeneity length scale  $a$ , and Hall-to-Ohmic resistivity ratio  $H$  of the normal conductor constituent satisfy the inequality  $H\ell \gg a$  (see Ref. 39).

### ACKNOWLEDGMENTS

This research was supported in part by grants from the US-Israel Binational Science Foundation, the Israel Science Foundation, and the KAMEA program of the Ministry of Absorption of the State of Israel.

### APPENDIX A: FREE-ELECTRON MODEL

#### 1. dc case

In a free-electron Drude model, the resistivity tensor  $\hat{\rho}_i$  and the conductivity tensor  $\hat{\sigma}_i = \hat{\rho}_i^{-1}$  can be written in the following forms

$$\hat{\rho}_i = \rho_0^{(i)} \begin{pmatrix} 1 & H_z^{(i)} & -H_y^{(i)} \\ -H_z^{(i)} & 1 & H_x^{(i)} \\ H_y^{(i)} & -H_x^{(i)} & 1 \end{pmatrix}, \quad (\text{A1})$$

$$\begin{aligned} \hat{\sigma}_i &= \frac{1}{\rho_0^{(i)}(1+H_i^2)} \\ &\times \begin{pmatrix} 1+(H_x^{(i)})^2 & H_x^{(i)}H_y^{(i)} & H_z^{(i)}H_x^{(i)} \\ H_x^{(i)}H_y^{(i)} & 1+(H_y^{(i)})^2 & H_y^{(i)}H_z^{(i)} \\ H_z^{(i)}H_x^{(i)} & H_y^{(i)}H_z^{(i)} & 1+(H_z^{(i)})^2 \end{pmatrix} \\ &+ \frac{1}{\rho_0^{(i)}(1+H_i^2)} \begin{pmatrix} 0 & H_z^{(i)} & -H_y^{(i)} \\ -H_z^{(i)} & 0 & H_x^{(i)} \\ H_y^{(i)} & -H_x^{(i)} & 0 \end{pmatrix}, \end{aligned} \quad (\text{A2})$$

where the Ohmic resistivity  $\rho_0^{(i)}$  is a scalar quantity independent of the magnetic field  $\mathbf{B}$ , while the Hall resistivity components  $\rho_0^{(i)}H_x^{(i)}$ ,  $\rho_0^{(i)}H_y^{(i)}$ ,  $\rho_0^{(i)}H_z^{(i)}$  form an axial vector that is proportional to  $\mathbf{B}$ . Consequently, the vector  $\mathbf{H}$  is a dimensionless form of the magnetic field whose magnitude is denoted by  $H \equiv \pm |\mathbf{H}| \equiv \pm \omega_c \tau$ , where  $\omega_c = e|\mathbf{B}|/mc$  is the cyclotron frequency, while  $\mathbf{B}$  is the magnetic field measured in conventional units, and  $\tau$  is the conductivity relaxation time. The sign of  $H$  can be either positive or negative, and reflects the sign of the majority charge carriers.

#### 2. ac case

The electrical permittivity tensors  $\hat{\epsilon}$  in a quasistatic approximation can be written as  $\hat{\epsilon} = \epsilon_0 \hat{I} + i(4\pi/\omega)\hat{\sigma}$ , where  $\omega$

is angular frequency,  $\epsilon_0$  is the scalar dielectric constant of the background ionic lattice, and  $\hat{I}$  is a unit tensor. The conductivity tensor  $\hat{\sigma}$  can be taken in the same forms as for dc case [see Eq. (A2)] but divided on  $(1-i\omega\tau)$  and the magnetic fields  $H$  should be substituted by  $H/(1-i\omega\tau)$ . Noting that  $\sigma_0 = N_0 e^2 \tau/m$  (here  $N_0$  is the charge-carrier density and  $m$  is electron mass) can be expressed through plasma frequency  $\omega_p = (4\pi e^2 N_0/m)^{1/2}$ , the local ac permittivity tensor  $\hat{\epsilon}$  of the metal for  $\mathbf{B} \parallel z$  can be written as<sup>29-31</sup>

$$\begin{aligned} \hat{\epsilon} &= \epsilon_0 \hat{I} + i\omega_p^2 \\ &\times \frac{\tau}{\omega} \begin{pmatrix} \frac{1-i\omega\tau}{(1-i\omega\tau)^2+H^2} & \frac{-H}{(1-i\omega\tau)^2+H^2} & 0 \\ \frac{H}{(1-i\omega\tau)^2+H^2} & \frac{1-i\omega\tau}{(1-i\omega\tau)^2+H^2} & 0 \\ 0 & 0 & \frac{1}{1-i\omega\tau} \end{pmatrix}. \end{aligned} \quad (\text{A3})$$

### APPENDIX B: DUALITY IN A 3D SYSTEM WITH COLUMNAR SYMMETRY

The current flow in a 3D medium with 2D heterogeneity, with the  $x$  axis as columnar symmetry axis (see Fig. 2), separates into a 1D problem for flow along that axis and a 2D problem for flow in the  $y,z$  plane when the constituent conductivity tensors have no elements connecting  $x$  to the other directions. That is the case for isotropic conductors when the externally applied magnetic field lies along  $x$ . By contrast, when one or more of the elements  $\mu_{xy}$ ,  $\mu_{yx}$ ,  $\mu_{xz}$ ,  $\mu_{zx}$  is nonzero, as when  $\mathbf{B}$  has a nonzero  $y$  or  $z$  component, the current flow becomes 3D in a nontrivial fashion. It was shown in Refs. 26 and 27, that the local fields  $\mathbf{J}$  and  $\mathbf{E}$  always depend only on  $y$  and  $z$  and also that  $E_x$  has a uniform value everywhere in the system. If the boundary conditions are such that  $E_x = 0$ , then Eqs. (2.1) and Eq. (2.2) both reduce to equations for a strictly 2D system which is just the  $y,z$  section of the columnar medium. Alternatively, one may define new potential fields by adding terms to  $\phi$  that are linear in  $y$  and  $z$  (see Refs. 16 and 40). Using either one of these approaches, the problem of calculating the four in-plane  $y,z$  tensor components of  $\hat{\mu}_e$  separates out from the full 3D problem and becomes a strictly 2D problem. Determination of the other five tensor components  $\mu_{xi}^{(e)}$  and  $\mu_{ix}^{(e)}$ ,  $i=x,y,z$ , is a separate problem. As shown in Refs. 28 and 41, in some cases the latter components are obtainable as linear combinations of the in-plane tensor components  $\mu_{\alpha\beta}^{(e)}$ ,  $\alpha,\beta=y,z$ .

It is therefore possible to define a dual 2D conductivity problem in the  $y,z$  plane: This is done by rotating the  $y$  and  $z$  components of  $\mathbf{E}$  and  $\mathbf{J}$  by  $90^\circ$  at every point in that plane, and calling the rotated fields  $\mathbf{J}_d$  and  $\mathbf{E}_d$ , respectively.<sup>2</sup> These are the dual current density or flux and dual electric field, and they satisfy the 2D equations  $\nabla \times \mathbf{E}_d = \nabla \cdot \mathbf{J}_d = 0$  in the  $y,z$  plane. From the relation



$$\mathbf{J}(\mathbf{r}) = \hat{\boldsymbol{\mu}}(\mathbf{r}) \cdot \mathbf{E}(\mathbf{r}), \quad \hat{\boldsymbol{\mu}} \equiv \begin{pmatrix} \mu_{yy} & \mu_{yz} \\ \mu_{zy} & \mu_{zz} \end{pmatrix}, \quad (\text{B1})$$

between the original 2D in-plane components of  $\mathbf{E}$  and  $\mathbf{J}$ , it follows that the dual fields are related by<sup>4</sup>

$$\mathbf{J}_d(\mathbf{r}) = \hat{\boldsymbol{\mu}}_d(\mathbf{r}) \cdot \mathbf{E}_d(\mathbf{r}), \quad (\text{B2})$$

$$\hat{\boldsymbol{\mu}}_d = \frac{1}{\det_{2D} \hat{\boldsymbol{\mu}}} \begin{pmatrix} \mu_{yy} & \mu_{zy} \\ \mu_{yz} & \mu_{zz} \end{pmatrix}. \quad (\text{B3})$$

A similar relation holds between the macroscopic 2D conductivity tensors of the original and dual problems, denoted by  $\hat{\boldsymbol{\mu}}_e$ ,  $\hat{\boldsymbol{\mu}}_d^{(e)}$

$$\hat{\boldsymbol{\mu}}_d^{(e)} = \frac{1}{\det_{2D} \hat{\boldsymbol{\mu}}_e} \begin{pmatrix} \mu_{yy}^{(e)} & \mu_{zy}^{(e)} \\ \mu_{yz}^{(e)} & \mu_{zz}^{(e)} \end{pmatrix}. \quad (\text{B4})$$

\*Electronic address: strelnik@ory.ph.biu.ac.il

†Electronic address: bergman@post.tau.ac.il

<sup>1</sup>J. B. Keller, *J. Math. Phys.* **5**, 548 (1964).

<sup>2</sup>A. M. Dykhne, *Zh. Éksp. Teor. Fiz.* **59**, 110 (1970) [*Sov. Phys. JETP* **32**, 63 (1971)].

<sup>3</sup>K. S. Mendelson, *J. Appl. Phys.* **46**, 917 (1975).

<sup>4</sup>K. S. Mendelson, *J. Appl. Phys.* **46**, 4740 (1975).

<sup>5</sup>B. I. Shklovskii, *Zh. Éksp. Teor. Fiz.* **72**, 288 (1977) [*Sov. Phys. JETP* **45**, 152 (1977)].

<sup>6</sup>D. Stroud and D. J. Bergman, *Phys. Rev. B* **30**, 447 (1984).

<sup>7</sup>G. W. Milton, *Phys. Rev.* **38**, 11 296 (1988).

<sup>8</sup>H. Christiansson, *Phys. Rev. B* **56**, 572 (1997).

<sup>9</sup>O. Levy and R. V. Kohn, *J. Stat. Phys.* **90**, 159 (1998).

<sup>10</sup>Y. Grabovsky, G. W. Milton, and D. S. Sage, *Commun. Pure Appl. Math.* **LIII**, 300 (2000).

<sup>11</sup>Y. Grabovsky and G. W. Milton, *Documenta Mathematica*, Extra Volume: ICM III, 623 (1998).

<sup>12</sup>A. M. Dykhne and I. M. Ruzin, *Phys. Rev. B* **50**, 2369 (1994).

<sup>13</sup>I. Ruzin and S. Feng, *Phys. Rev. Lett.* **74**, 154 (1995).

<sup>14</sup>K. Schulgasser, *J. Math. Phys.* **17**, 378 (1975).

<sup>15</sup>D. J. Bergman, *Ann. Phys. (N.Y.)* **138**, 78 (1982).

<sup>16</sup>Y. M. Strelniker and D. J. Bergman, *Phys. Rev. B* **61**, 6288 (2000).

<sup>17</sup>D. J. Bergman and Y. M. Strelniker, *Phys. Rev. B* **62**, 14 313 (2000).

<sup>18</sup>The bulk effective magnetoconductivity tensor components were calculated using the numerical approach developed and described in Refs. 19–21. The efficiency of this approach is verified and demonstrated in comparison with the other numerical calculations (Ref. 22) as well as with results of the real experiments (Refs. 23 and 24).

<sup>19</sup>Y. M. Strelniker and D. J. Bergman, *Phys. Rev. B* **50**, 14 001 (1994).

<sup>20</sup>Y. M. Strelniker and D. J. Bergman, *Phys. Rev. B* **53**, 11 051 (1996).

<sup>21</sup>D. J. Bergman and Y. M. Strelniker, *Phys. Rev. B* **49**, 16 256 (1994).

<sup>22</sup>K. D. Fisher and D. Stroud, *Phys. Rev. B* **56**, 14 366 (1998).

<sup>23</sup>M. Tornow, D. Weiss, K. v. Klitzing, K. Eberl, D. J. Bergman, and

Y. M. Strelniker, *Phys. Rev. Lett.* **77**, 147 (1996).

<sup>24</sup>G. J. Strijkers, F. Y. Yang, D. H. Reich, C. L. Chien, P. C. Searson, Y. M. Strelniker, and D. J. Bergman, *IEEE Trans. Magn.* **37**, 2067 (2001).

<sup>25</sup>D. J. Bergman and Y. M. Strelniker, *Superlattices Microstruct.* **23**, 547 (1998); special issue dedicated to Rolf Landauer on the occasion of his 70th birthday.

<sup>26</sup>D. J. Bergman and Y. M. Strelniker, *Phys. Rev. Lett.* **80**, 3356 (1998).

<sup>27</sup>D. J. Bergman and Y. M. Strelniker, *Phys. Rev. B* **59**, 2180 (1999).

<sup>28</sup>D. J. Bergman and Y. M. Strelniker, *Phys. Rev. B* **60**, 13 016 (1999).

<sup>29</sup>Y. M. Strelniker and D. J. Bergman, *Phys. Rev. B* **59**, R12 763 (1999).

<sup>30</sup>D. J. Bergman and Y. M. Strelniker, *Phys. Rev. Lett.* **80**, 857 (1998).

<sup>31</sup>Y. M. Strelniker and D. J. Bergman, *Eur. Phys. J.: Appl. Phys.* **7**, 19 (1999).

<sup>32</sup>T. W. Ebbesen, H. J. Lezec, H. F. Ghaemi, T. Thio, and P. A. Wolf, *Nature (London)* **391**, 667 (1998).

<sup>33</sup>V. G. Veselago, *Usp. Fiz. Nauk* **92**, 517 (1967) [*Sov. Phys. Usp.* **10**, 509 (1968)].

<sup>34</sup>J. B. Pendry, *Phys. Rev. Lett.* **85**, 3966 (2000).

<sup>35</sup>D. R. Smith, S. Schultz, P. Markos, and C. M. Soukoulis, *Phys. Rev. B* **65**, 195 104 (2002).

<sup>36</sup>A. L. Pokrovsky and A. L. Efros, *Phys. Rev. Lett.* **89**, 093 901 (2002).

<sup>37</sup>E. Yablonovitch, T. J. Gmitter, and K. M. Leung, *Phys. Rev. Lett.* **67**, 2295 (1991).

<sup>38</sup>K. M. Ho, C. T. Chan, and C. M. Soukoulis, *Phys. Rev. Lett.* **65**, 3152 (1990).

<sup>39</sup>D. J. Bergman and Y. M. Strelniker, *Phys. Rev. B* **51**, 13 845 (1995).

<sup>40</sup>Y. M. Strelniker and D. J. Bergman, in *Physics of Semiconductors 2002: Proceedings of the 26th International Conference on the Physics of Semiconductors (ICDS26)*, Edinburgh, 2002, Institute of Physics Conference Series No. 171, edited by A. R. Long and J.H. Davies (Institute of Physics, Bristol, 2003).

<sup>41</sup>D. J. Bergman and Y. M. Strelniker (unpublished).